International Journal of Electrical and Computer Engineering (IJECE)
Vol.1, No.2, December 2011, pp. 119~134
ISSN: 2088-8708

Smoothing Control of Wind Farm Output Fluctuations by Fuzzy Logic Controlled SMES

M.R.I. Sheikh[#1], and J. Tamura[*2]
[#1]EEE Department, Rajshahi University of Engineering & Technology
Rajshahi – 6204, Bangladesh
[#1]EEE Department, Kitami Institute of Technology
165 koen-cho, Hokkaido, kitami 090-8507, Japan
[1]Emai: ris_ruet@yahoo.com

Abstract

Due to random variations of wind speed, the output power and terminal voltage of a fixed speed wind generator fluctuate continuously. These irregularities in power output are affecting both the power quality and reliability. It is reported that STATCOM/SMES (Superconducting Magnetic Energy Storage) system can significantly decrease voltage and output power fluctuations of grid connected fixed speed wind generator. But the main problem in wind generator output power smoothing is the choice of the reference output power, because it corresponds to energy storage capacity. The storage capacity of SMES that is sufficient for the smoothing control but as small as possible is very important, considering cost effectiveness. In this paper, a fuzzy logic controlled STATCOM/SMES system is proposed, in which both SMA (Simple Moving Average) and EMA (Exponential Moving Average) are used to generate output power reference. Real wind speed data are used in the simulation analyses, which validate the effectiveness of the proposed control strategy. Simulation results clearly show that the proposed STATCOM/SMES system can smooth well the wind generator output power and also maintain the terminal voltage at rated level in both cases when SMA or EMA is used to generate output reference power. Finally, it is shown that reference output power generated by EMA provides better performance with reduced SMES storage capacity than that of output power generated by SMA.

Keywords*: Minimization of fluctuations, fixed speed wind generator, STATCOM/SMES, simple moving average (SMA) and exponential moving average (EMA), and wind farm (WF).*

Nomenclature

A. Symbols and subscripts

R_a	armature resistance
X_a	armature reactance
X_d	direct-axis synchronous reactance
X_q	quadrature-axis synchronous reactance
X'_d	direct-axis transient reactance
X'_q	quadrature-axis transient reactance
X''_d	direct-axis subtransient reactance
X''_q	quadrature-axis subtransient reactance
T'_{d0}	direct-axis open circuit transient time constant
T''_{d0}	direct-axis open circuit subtransient time constant
T''_{q0}	quadrature-axis open circuit subtransient time constant
H	inertia constant
r_1	stator resistance
x_1	stator reactance
X_{mu}	magnetizing reactance
r_{21}	rotor 1st cage resistance
x_{21}	rotor 1st cage reactance
r_{22}	rotor 2nd cage resistance
x_{22}	rotor 2nd cage reactance
P_{WF}	extracted power from the wind farm
T_w	turbine torque
ρ	air density
R	blade radius
V_w	wind speed
C_p	power co-efficient
λ	tip speed ratio
β	blade pitch angle
ω_B	blade angular velocity
E	inductively stored energy
L_{sm}	inductance of the coil

Received Sep 11th, 2011; Revised Nov 14th, 2011; Accepted Nov 24th, 2011

I_{sm} DC current flowing through the coil
V_{sm} voltage across the coil
$\bar{I}$ phasor quantity of the current flowing from ac system side to the converter side
I_d real component of $\bar{I}$
I_q imaginary component of $\bar{I}$
V_d real component of the VSC output ac voltage
V_q imaginary component of the VSC output ac voltage
D chopper duty cycle
V_L wind farm terminal voltage
V_{L_ref} wind farm terminal reference voltage
V_{dc} dc link voltage
V_{dc_ref} dc link reference voltage
$I_{a,b,c}$ I_a, I_b, I_c
$V_{a,b,c}$ V_a, V_b, V_c
P_G wind generator real power
Q_G wind generator reactive power
P_{ref} wind farm line reference real power

1. Introduction

Due to the degradation and cost increase of conventional fuel and also the environmental problem such as global warming, it is necessary to introduce clean energy more in place of the fossil fuel. Because of the reason of almost no carbon dioxide (CO2) emission, wind energy, solar energy, biomass, etc. have attracted the attention remarkably in the world due to their clean energy characteristics. These energy sources are renewable, and the exhaustion problem of fossil fuel makes those prospective and alternate energy sources of the future world. Among the renewable energy sources stated above, wind power generation has some merits as follows: 1) its efficiency is relatively high, 2) installation cost per unit output can be decreased by adopting a wind generator with large power capacity, 3) it can receive some political support for installation, and so on. Although wind power is considered as a very prospective clean energy source, wind power fluctuation caused by randomly varying wind speed is still a serious problem for power grid companies or transmission system owners (TSOs), especially in the case of fixed-speed wind generators. Induction generators (IGs) are used, in general, as fixed-speed wind generator because of their superior characteristics such as brushless and rugged construction, low cost, maintenance and operational simplicities. However, during startup, the induction generators need reactive power. As the reactive power drained by the induction generators is coupled to the active power generated by them, the variation of wind speed causes the variations of IGs real and reactive powers. These active and reactive power variations interact with the network and thus initiate voltage and frequency fluctuations. Therefore, smoothing control of wind turbine generator output fluctuations is very important from a point of view of power system security, especially for power system frequency. With these points as background, it is a very effective method to suppress these fluctuations by using fast acting energy storage system [1].

Recently, FACTS with energy storage system (ESS) have emerged as promising devices for power system applications [2-4]. Every system has some merits and demerits. Another alternate and effective method among various energy storage systems is SMES (Superconducting Magnetic Energy Storage) [5-7]. The SMES is a large superconducting coil capable of storing electric energy in the magnetic field generated by dc current flowing through it. Since the successful commissioning test of the Bonneville Power Administration (BPA) 30 MJ unit [8], SMES systems have received much attention in power system applications, such as diurnal load demand leveling, frequency control, automatic generation control, uninterruptible power supplies, etc. Due to high response speed it is capable of quickly releasing megawatt amounts of power. The real power as well as the reactive power can be absorbed by or released from the SMES unit according to the system power requirements. The ability of injecting/absorbing real or reactive power can increase the effectiveness of the control, provide operation flexibility and enhance system reliability, and thus the SMES can be a prospective option in building a FACTs.

In our previous study we have proposed a method [9], however this paper proposes a model of a STATCOM/SMES system and its control algorithm by using fuzzy logic controller to decrease voltage and output power fluctuations effectively of fixed speed wind generator during random wind speed variations. The control scheme of SMES is based on a pulse width modulation (PWM) voltage source converter (VSC) and a two-quadrant DC-DC chopper using an insulated-gate bipolar transistor (IGBT). Charge and discharge of SMES are determined by the chopper duty cycle, which is controlled by fuzzy logic. Therefore, the SMES is capable of controlling both active and reactive powers simultaneously, independently, and quickly [10-12]. It is also expected that large SMES capacity give better smoothing performance. However, large capacity will definitely increase the system overall cost, making the installation of SMES impractical. Considering this veiwpoint, reference output power is generated by using both SMA and EMA. Finally, comparative results with enough smoothing effect have been presented. It is seen that the proposed control system can smooth the wind farm output power as well as maintain constant voltage

magnitude at wind farm terminal in both cases with the two power references used. But reference power generated by EMA is considered more effective with both reduced SMES real power and energy storage capacity. This is the salient feature of this paper. Considering these viewpoints, this paper proposes a novel control strategy of the STATCOM/SMES installed at a wind farm for decreasing fluctuations of output power and terminal voltage of grid connected wind farm.

2. Model System

The model system as shown in Fig. 1 is considered for the simulation of wind generator stabilization in this work. The model system consists of one synchronous generator (100MVA), SG, and a wind farm (WF) model consisting of five wind generators (10MVA×5=50 MVA), which are delivering power to an infinite bus through a transmission line with two circuits. There is a local transmission line with one circuit between the main transmission line and the transformers at the wind power station. The double squirrel-cage induction machine model, which is represented by a steady state equivalent circuit shown in Fig. 2 where s denotes a rotational slip, is used for the wind generators. To establish the rotating magnetic field of the stator, reactive power is needed to be supplied from the network to the stator winding of the induction generators (IGs). So, to compensate the reactive power demand at steady state, a capacitor bank is inserted at the terminal of IG [13-15]. The value of the capacitor C is so chosen that the power factor of the wind power station becomes unity when it is operating in the rated condition (V=1.0, P=0.5). The SMES unit is located at the wind farm terminal bus. The AVR (Automatic Voltage Regulator) and GOV (Governor) control system models shown in Fig. 3 and Fig. 4 respectively are used in the synchronous generator model. The parameters of generator and initial conditions [15] are shown in Table I and Table II respectively. The system base power is 100 MVA.

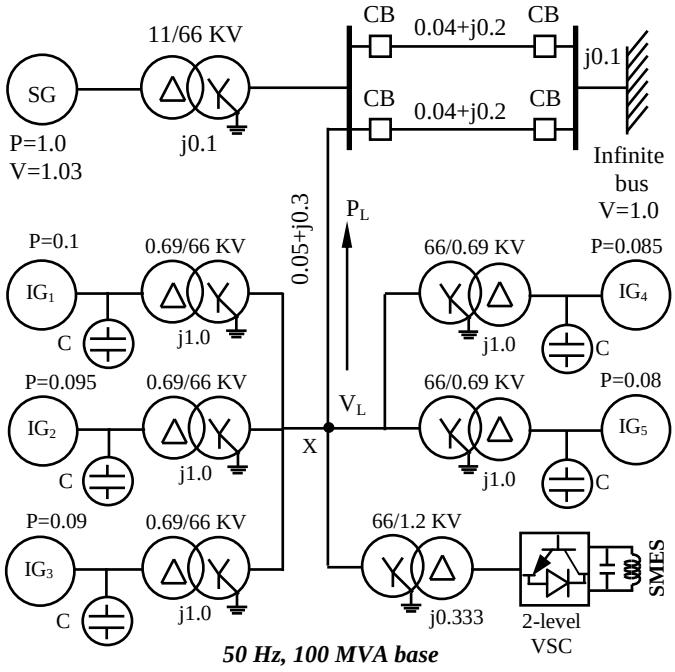

Fig. 1. Power system model with STATCOM/SMES

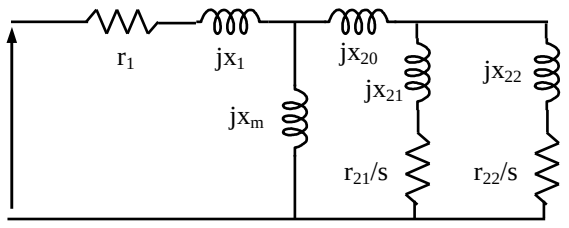

Fig. 2. Steady state equivalent circuit of double squirrel-case induction generator

Table I
Generator Parameters

SG		IG	
MVA	100	MVA	50
Ra(pu)	0.003	r1(pu)	0.01
Xa(pu)	0.13	x1(pu)	0.1
Xd(pu)	1.2	Xmu(pu)	3.5
Xq(pu)	0.7	r21(pu)	0.035
Xd′(pu)	0.3	x21(pu)	0.030
Xq′(pu)	0.22	r22(pu)	0.014
Xd″(pu)	0.22	x22(pu)	0.098
Xq″(pu)	0.25	H(sec)	1.5
Td0′(sec)	5.0		
Td0″(sec)	0.04		
Tq0″(sec)	0.05		
H(sec)	2.5		

Table II
Initial Conditions

	SG	IG_1	IG_2	IG_3	IG_4	IG_5
P(pu)	1.0	0.10	0.095	0.09	0.085	0.08
V(pu)	1.03	1.017	1.019	1.022	1.024	1.026
Q(pu)	0.289	0.001 (0.048*)	0.003 (0.046*)	0.005 (0.044*)	0.007 (0.043*)	0.009 (0.041*)
E_{fd}(pu)	1.761	-	-	-	-	-
Tm(pu)	1.003	-	-	-	-	-
δ(deg)	50.64	-	-	-	-	-
slip	0.0	-1.05%	-0.99%	-0.93%	-0.87%	-0.81%
V_w(m/s)	-	11.795	11.525	11.257	10.99	10.7233
β(deg)	-	0	0	0	0	0

*Reactive power drawn by induction generator

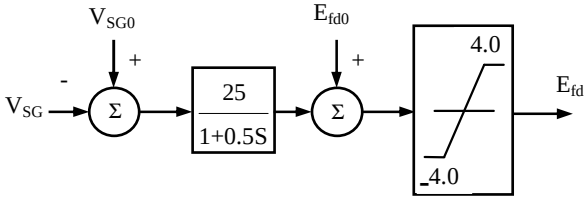

Fig. 3. AVR Model

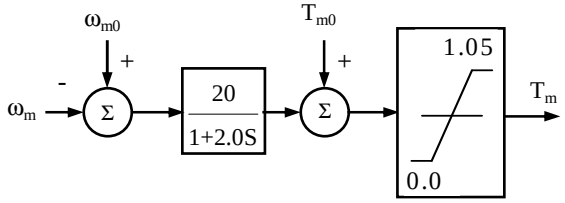

Fig. 4. GOV Model

3. Modeling of Wind Turbine

The model of wind turbine rotor is complicated. According to the blade element theory [16], modeling of blade and shaft needs complicated and lengthy computations. Moreover, it also needs detailed and accurate information about rotor geometry. For that reason, considering only the electrical behavior of the system, a simplified method of modeling of the wind turbine blade and shaft is normally used. The mathematical relation for the mechanical power extraction from the wind can be expressed as follows:

$$P_w = 0.5\rho\pi R^2 V_w^3 Cp(\beta, \lambda) \quad (1)$$

Where, P_w, is the extracted power from the wind, ρ is the air density [kg/m^3], R is the blade radius[m] and C_p is the power coefficient which is a function of both tip speed ratio, λ, and blade pitch angle, β[deg]. The C_p equation has been taken from [17].

$$\lambda = \frac{V_w}{\omega_B} \tag{2}$$

$$C_p = \frac{1}{2}\left(\lambda - 0.022\beta^2 - 5.6\right)e^{-0.17\lambda} \tag{3}$$

Where, ω_B is the rotational speed of turbine hub [rad/s]. Here wind speed, V_w, is in mile/hr. The C_p-λ curves are shown in Fig. 5 for different values of β. Power versus wind speed characteristic is also shown in Fig. 6. When the wind velocity exceeds the rated speed, then the pitch angle of the blade needs to be controlled to maintain the output at the rated level. Fig. 6 also shows the control of pitch angle with the variation of wind velocity to control the output power nearly constant at rated capacity. Now the turbine torque, T_w, can be calculated from (4).

$$T_w = 0.5\rho\pi R^2 V_w^2 Cp(\beta,\lambda)/\lambda \tag{4}$$

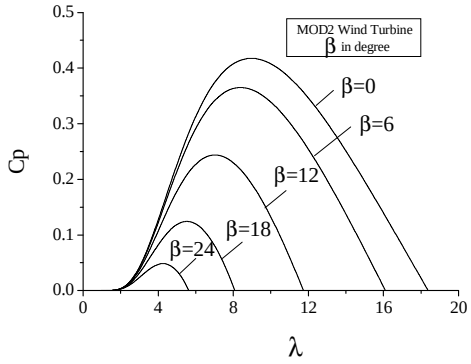

Fig. 5. C_P- λ curves for different pitch angles

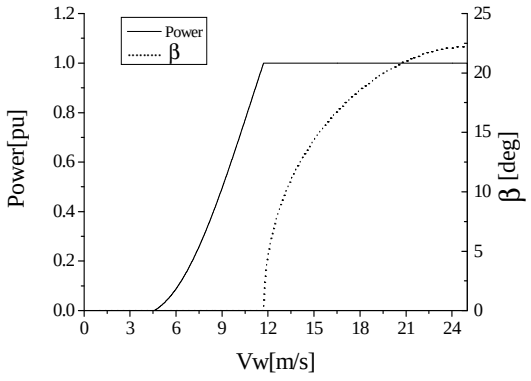

Fig. 6. Output power versus wind speed and pitch angle versus wind speed characteristics

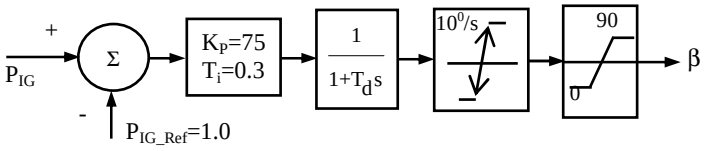

Fig. 7. Pitch angle controller

The pitch angle is controlled to maintain the output power at rated value when the wind speed is over the rated one. The pitch servo shown in Fig. 7 is modeled with a first order delay system with a time constant T_d=5 sec. Because the pitch actuation system cannot, in general, respond instantly, a rate limiter with a value of 10^0/sec is added.

4. STATCOM/SMES Topology

4.1. Brief Overview of SMES System

The SMES system used in this study consists of a wye-delta transformer, a 6-pulse PWM voltage source converter (VSC) using IGBT, a DC link capacitor, a two-quadrant DC-DC chopper using IGBT, and a superconducting coil. The detailed switching model is considered in the SMES modeling instead of time-averaged model and hence losses in the power converters are taken into consideration, in this study. The VSC and the DC-DC chopper are linked by a DC link capacitor of 50 mF. The rated DC link voltage is 2 kV, which is kept constant throughout. The SMES is coupled to the 66 kV line through a single step-down transformer (66/1.2 kV) with 0.333 pu leakage reactance (based on 100 MVA base value).

For a SMES system, the inductively stored energy (E in Joule) and the rated power (P in Watt) are commonly the given specifications for SMES devices, and can be expressed as follows:

$$E = \frac{1}{2} I_{sm}^2 L_{sm} \tag{5}$$

$$P = \frac{dE}{dt} = L_{sm} I_{sm} \frac{dI_{sm}}{dt} = V_{sm} I_{sm} \tag{6}$$

where L_{sm} is the inductance of the coil, I_{sm} is the DC current flowing through the coil, and V_{sm} is the voltage across the coil. The proposed SMES has the power rating and energy capacity of 30 MW and 0.5 MWh respectively.

4.2. PWM Voltage Source Converter (VSC)

In this study, the well-known cascade control scheme with independent control of the active and reactive currents was developed for the voltage source converter as shown in Fig. 8. Suitable adjustment of phase and magnitude of the VSC output voltage allows effective control of power exchange between SMES and the ac system. The SMES is used also to regulate the WF terminal voltage. Therefore, the aim of the control is to maintain the magnitude of voltage at the WF terminal to be at the desired level. The DC link voltage (V_{dc}) is also kept constant at the rated value. Finally, the three-phase reference signals are compared with the triangular carrier wave signal in order to generate the switching signals for the IGBT-switched VSC. In this study, the interpolated firing pulses are used in sinusoidal PWM controller. The interpolated firing pulse circuit is a simulation technique concerned with generating firing pulses through interpolation procedure. This allows for exact switching between time steps based on a comparison between the sinusoidal reference and the high-frequency carrier signal. High switching frequencies can be used to improve the efficiency of the converter, without incurring significant switching losses. In the simulation analyses, the switching frequency is chosen 1000 Hz. The snubber circuit resistance and capacitance values of the IGBT devices are 5000 Ω and 0.05 μF respectively.

4.3. Two-Quadrant DC-DC Chopper

Depending upon the values of chopper duty cycle D, three regions of operation can be identified for the chopper arrangement of Fig. 9(a). The timing diagrams pertaining to these regions of operation are shown in Fig. 9(b), in which for charge/discharge/standby operation, the value of S=+1/-1/0. It is clear from Fig. 9(b) that average voltage appearing across the SMES coil and chopper current at any instant of time can be represented by (7),

$$\begin{aligned} V_{SM\_av} &= [1-2D]V_{dc\_av} \\ I_{dc\_av} &= [1-2D]I_{SM\_av} \end{aligned} \tag{7}$$

where V_{SM_av} is the average voltage across the SMES coil, I_{SM_av} is the average current through the SMES coil, V_{dc_av} is the average dc source voltage, I_{dc_av} is the average dc source current, and D is the duty cycle of the chopper (D=IGBT conduction time/period of one switching cycle).

The superconducting coil is charged or discharged by adjusting the average (i.e., dc) voltage across the coil to be positive or negative values by means of the dc-dc chopper duty cycle D controlled by the fuzzy logic controller (FLC). When the duty cycle is larger than 0.5 or less than 0.5, the coil is either charging or discharging respectively. When the unit is on standby, the coil current is kept constant, independent of the storage level, by adjusting the chopper duty cycle to 50%, resulting in the net voltage across the superconducting winding to be zero.

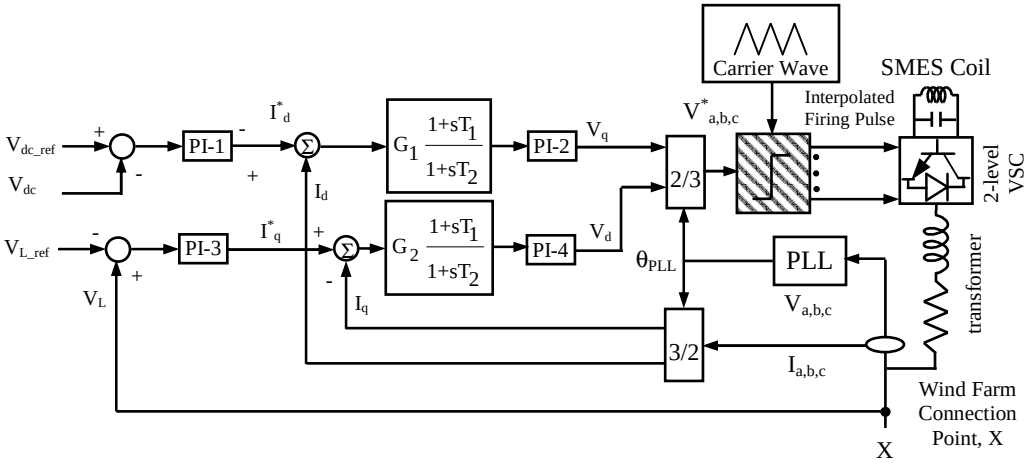

Fig. 8. Control system of the VSC

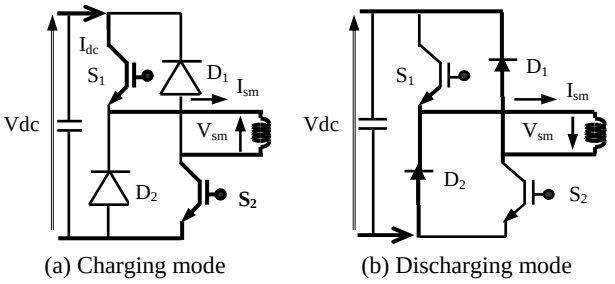

Fig. 9(a). The control concept of SMES charging and discharging

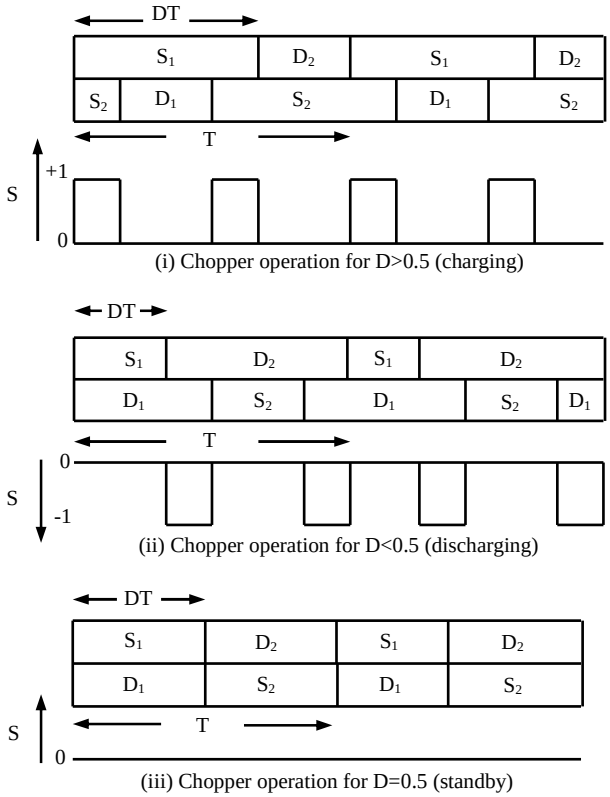

Fig. 9(b). Details of switching positions for corresponding chopper operation

Table III
Parameters of PI Controllers

	PI-1	PI-2	PI-3	PI-4
K_P	1.0	0.1	1.0	0.1
T_i	0.02	0.002	0.02	0.002

In order to generate the gate signals for the IGBT's of the chopper, the PWM reference signal is compared with the saw tooth carrier signal as shown in Fig. 10. The frequency of the saw tooth carrier signal for the chopper is chosen 100 Hz. The parameters of the PI controllers used in Fig. 8 are shown in Table III.

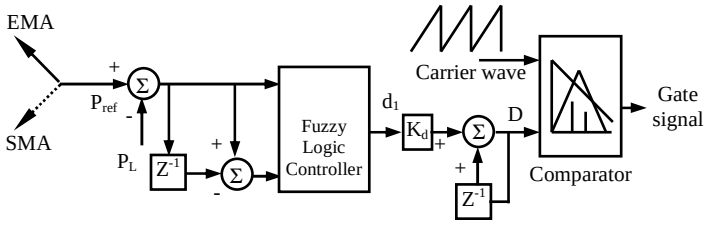

Fig. 10. Control system of two-quadrant dc-dc chopper

4.4. Generation of Line Power Reference, P_{ref}

WF output power reference signal, P_{ref}, is generated by the following ways:

(i) SMA: The n period SMA[15] for period d is computed by:

$$SMA_d = \frac{\sum_{i=1}^{n} M_{(d-i)+1}}{n}; \ (n \le d) \tag{8}$$

If ten measurements, M_1 through M_{10} are available, the successive 4 period simple moving average, for example, are as follows:

$$\begin{aligned} SMA_4&=(M_4+M_3+M_2+M_1)/4 \\ SMA_5&=(M_5+M_4+M_3+M_2)/4 \\ &\cdot \\ &\cdot \\ SMA_{10}&=(M_{10}+M_9+M_8+M_7)/4 \end{aligned} \tag{9}$$

It is not possible to compute a 4 period moving average until 4 periods data are available. That's why the first moving average in the above example is SMA_4.

(ii) EMA: N periods EMA[15] is calculated using the formula shown below.

$$EMA(C)=[(C-P)\times K]+P \tag{10}$$

where C= current value, P= previous period's EMA and K= weighting factor. For a period-based EMA, "K" is equal to 2 /(1 + N), where N is the specified number of periods. For example, a 10-period EMA's "weighting factor" is calculated like this: 2/(1+10)=0.1818.

5. Fuzzy Logic Controller Design

The proposed FLC system as shown in Fig. 10 is used to find out the duty cycle, D, in the control block from the error signal, e, and change of error signal, Δe. The FLC is explained in the following:

5.1. Fuzzification

To design the proposed FLC, the error signal, e(k), and change of error signal, Δe(k) are considered as the controller inputs. Considering these two inputs, the output (duty cycle), D is determined. The use of two input and single output variable makes the design of the controller very straightforward. In this work, the scaling factor K_d is considered as constant and the value is determined by trial and error method for better performance. In Fig. 10, Z^{-1} represents one sampling time delay. The triangular membership functions used for the input and output fuzzy set are

shown in Fig. 11, in which the linguistic variables are represented by Negative Big (NB), Negative Small (NS), Zero (Z), Positive Small (PS), and Positive Big (PB). A membership value for the various linguistic variables is calculated by the rule given by

$$\mu\left(e_k,\Delta e_k\right)=\min\left[\mu\left(e_k\right),\mu\left(\Delta e_k\right)\right] \tag{11}$$

5.2. Fuzzy Rule Base

The fuzzy mapping of the input variables to the output is represented by "IF-THEN" rules. In the work, we have developed 25 simple control rules corresponding to 5 linguistic variables NB, NS, Z, PS and PB for the fuzzy controller design. These are as follows:

IF <e(k) is Z> AND <Δe(k) is NB> THEN <d_1(k) is NS>
IF <e(k) is PB> AND <Δe(k) is PB> THEN <d_1(k) is PB>

5.3. Inference Mechanism

For the inference mechanism of the proposed fuzzy logic controller, Mamdani's method [18] has been utilized. According to Mamdani, the equation of the triangular membership function used to determine the grade of membership values in this work is as follows:

$$A\left(x\right)=\frac{\left(b-2\left|x-a\right|\right)}{b} \tag{12}$$

where A(x) is the value of grade of membership, 'b' is the width and 'a' is the coordinate of the point at which the grade of membership is 1 and x is the value of the input variables. The control rules for the proposed strategy are very straightforward and have been developed from the viewpoint of practical system operation and by trial and error methods. The entire rule base is given in Table IV.

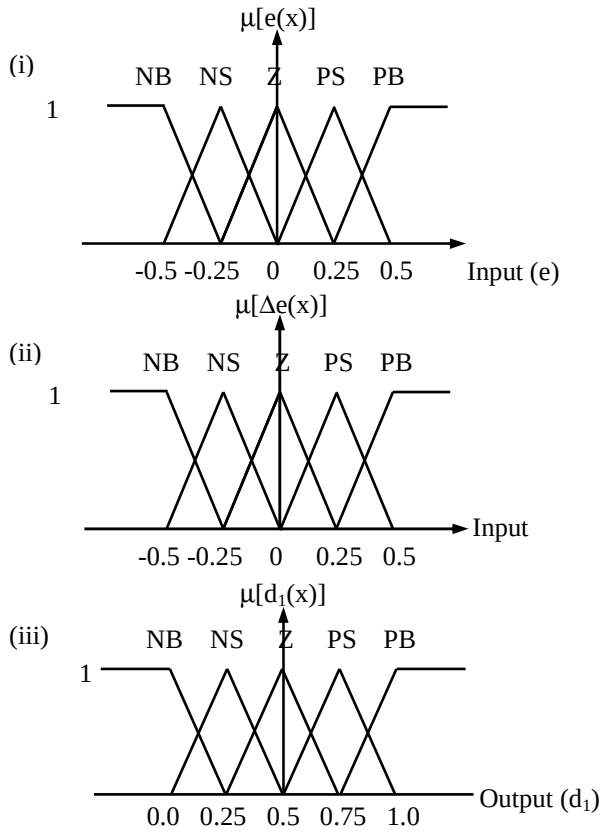

Fig. 11. Fuzzy sets and their corresponding membership functions

Table IV
Fuzzy Rule Table

d_1		Δe				
		NB	NS	Z	PS	PB
e	NB	NB	NB	NS	NS	Z
	NS	NB	NS	NS	Z	PS
	Z	NS	NS	Z	PS	PS
	PS	NS	Z	PS	PS	PB
	PB	Z	PS	PS	PB	PB

5.4. Defuzzification

The center-of-gravity method is the most well-known and rather simple defuzzification method [18], which is implemented to determine the output (d_1). This is given by the following expression

$$d_1 = \frac{\sum_{j=1}^{n} \mu_j u_j}{\sum_{j=1}^{n} \mu_j} \tag{13}$$

where n is the total number of rules, μ_i is the membership grade for i^{th} rule and u_j is the coordinate corresponding to the respective output (crispy value in the fuzzy rule table).

6. Simulation Results

To verify the effectiveness of the proposed control system, two different patterns of real wind speed data, which were obtained in Hokkaido Island, Japan, are used in the simulation analyses. The time step and simulation time have been chosen 0.00001sec and 600 sec respectively. The simulations have been done by using PSCAD/EMTDC [19]. Two cases are considered to show the effectiveness of STATCOM/SMES topology for WF output power and terminal voltage smoothing.

Case I: SMA is used to generate WF output power reference.
Case II: EMA is used to generate WF output power reference.

6.1. Simulation using widely varying wind speed data

In this case, wind pattern with wide variations shown in Fig. 12 was used in all the IGs. Fig. 13 and Fig. 14 show the WF terminal voltage and WF real power responses without STATCOM/SMES respectively. It is seen that when there is no STATCOM/SMES WF cannot maintain the terminal voltage constant and also cannot smooth the wind farm line power output. Fig. 14 also shows the WF line power responses for both cases when STATCOM/SMES is connected to WF terminal. It is clear from Fig. 14 that the STATCOM/SMES can smooth the WF line power well in both cases. Fig. 15 shows the real power compensation from the STATCOM/SMES for both cases. But comparatively more compensation is required in case I. In Fig. 16, WF terminal voltage responses are presented for both cases when STATCOM/SMES is used. It is seen that STATCOM/SMES can maintain the terminal voltage constant in both cases. Fig. 17 and Fig. 18 show the responses of SMES reactive power and SMES stored energy respectively. It is also clear from Fig. 17 and Fig. 18 that more reactive power compensation and larger SMES energy storage capacity are needed in case I than Case II.

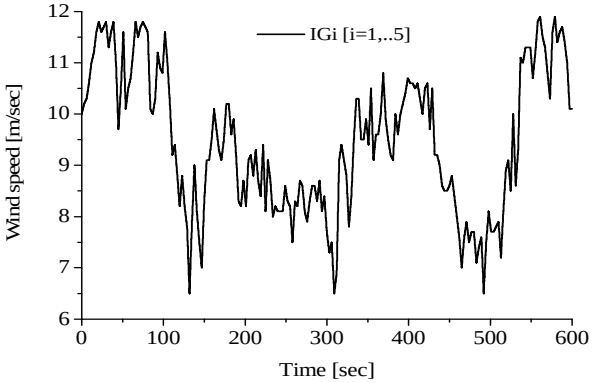

Fig. 12. Response of real wind data

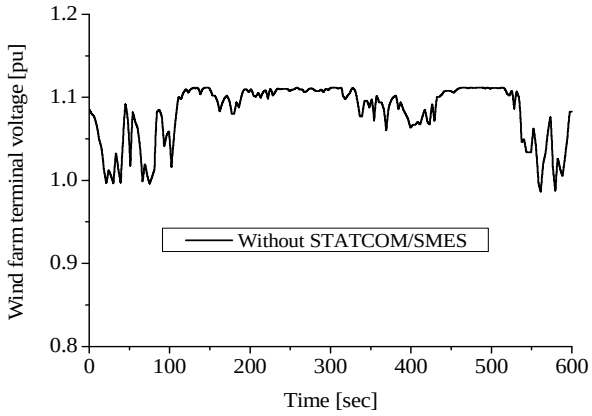

Fig. 13. Terminal voltage response of WF without STATCOM/SMES

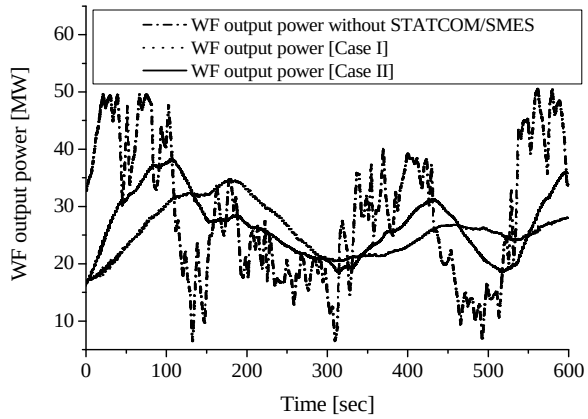

Fig. 14. Responses of WF output power with and without STATCOM/SMES

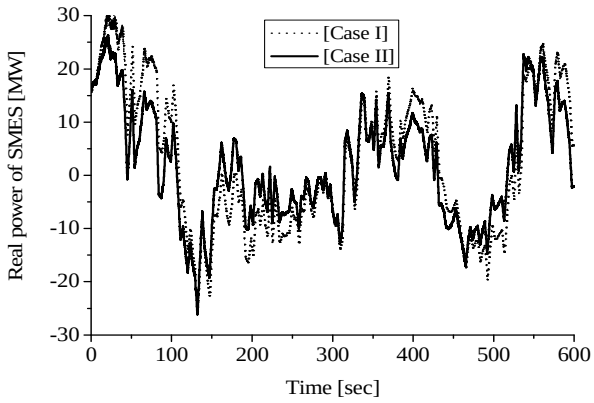

Fig. 15. Responses of SMES real power

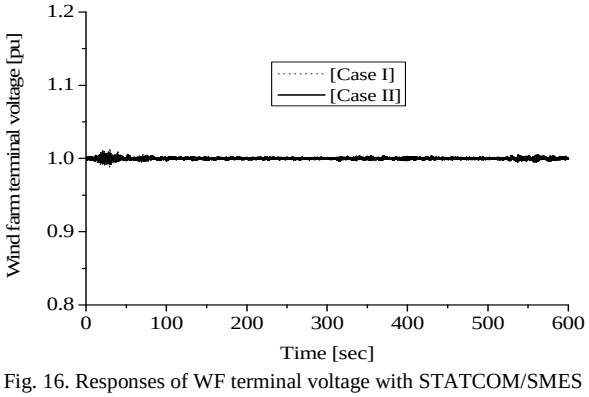

Fig. 16. Responses of WF terminal voltage with STATCOM/SMES

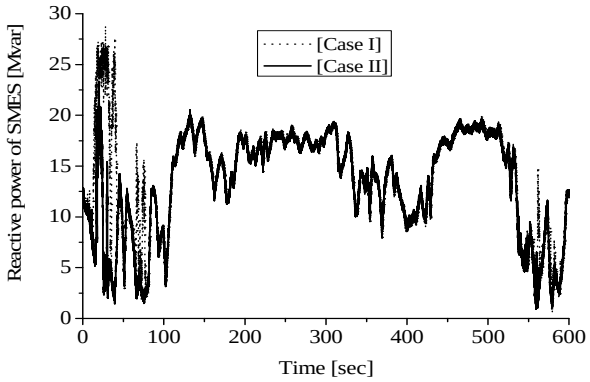

Fig. 17. Responses of SMES reactive power

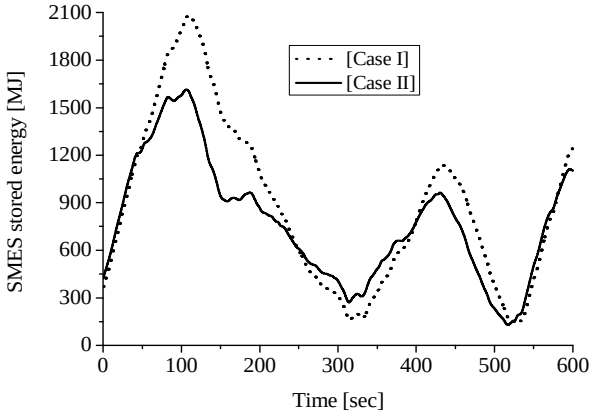

Fig. 18. Responses of SMES energy

6.2. Simulation using moderate wind speed data

In this case, moderate wind speed pattern as shown in Fig. 19 is also used in all IGs. Fig. 20 and Fig. 21 show the WF terminal voltage and WF real power responses without STATCOM/SMES respectively. It is seen that only conventional pitch controller cannot regulate the terminal voltage constant and also cannot smooth well the wind farm line power output, when there is no STATCOM/SMES connected. Fig. 22 shows that blade pitch angle. Fig. 21 also shows the WF line power responses for both cases when STATCOM/SMES is connected to WF terminal. For this wind data, it is also clear from Fig. 21 that the STATCOM/SMES can smooth the WF line power well in both cases. Fig. 23 shows the real power compensation from the STATCOM/SMES for both cases. But comparatively more compensation is required in case I. In Fig. 24, WF terminal voltage responses are presented for both cases when STATCOM/SMES is used. It is also seen that STATCOM/SMES can maintain the terminal voltage constant in both cases.

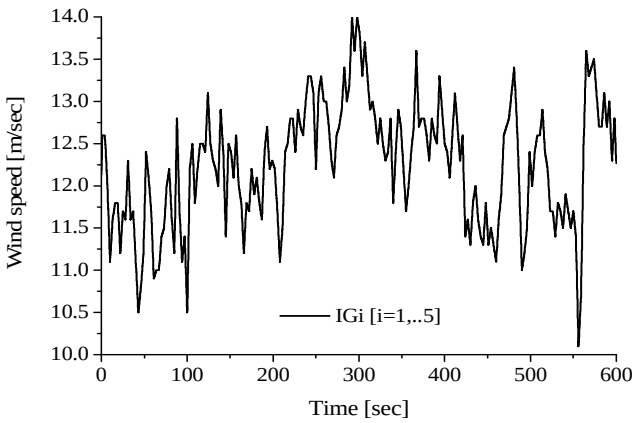

Fig. 19. Response of real wind data

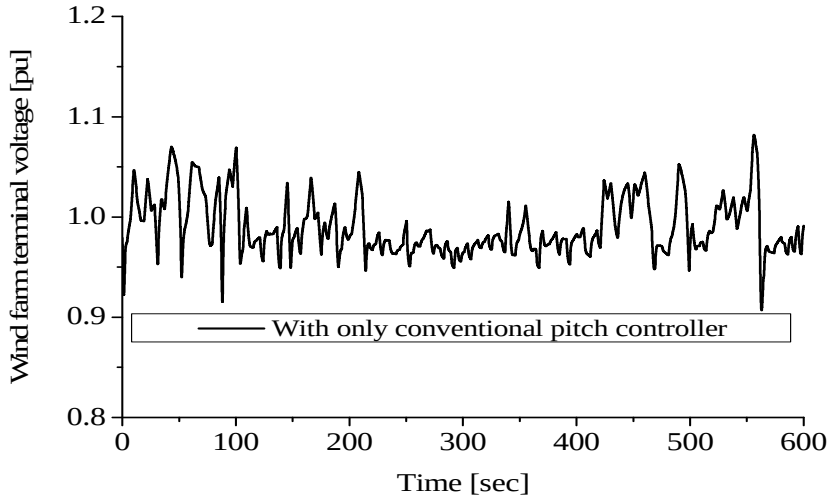

Fig. 20. Terminal voltage response of WF without STATCOM/SMES

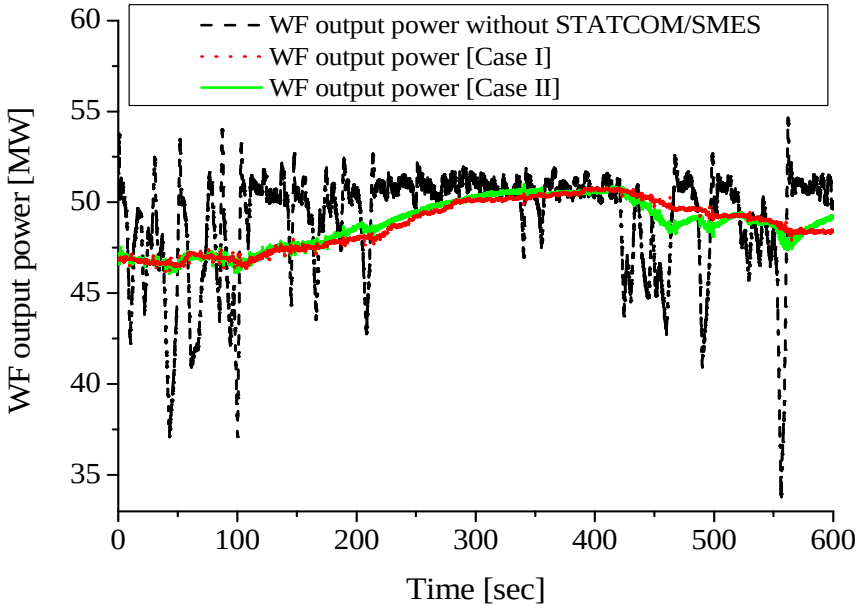

Fig. 21. Responses of WF line power with and without STATCOM/SMES

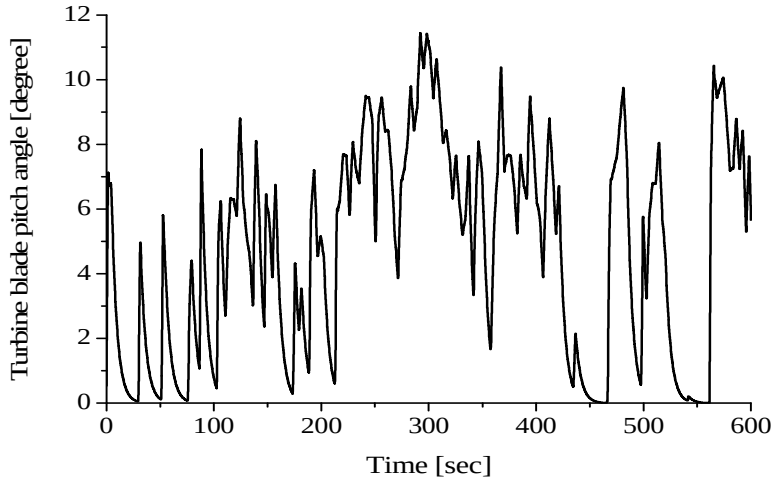

Fig. 22. Response of turbine (IG1) blade pitch angle

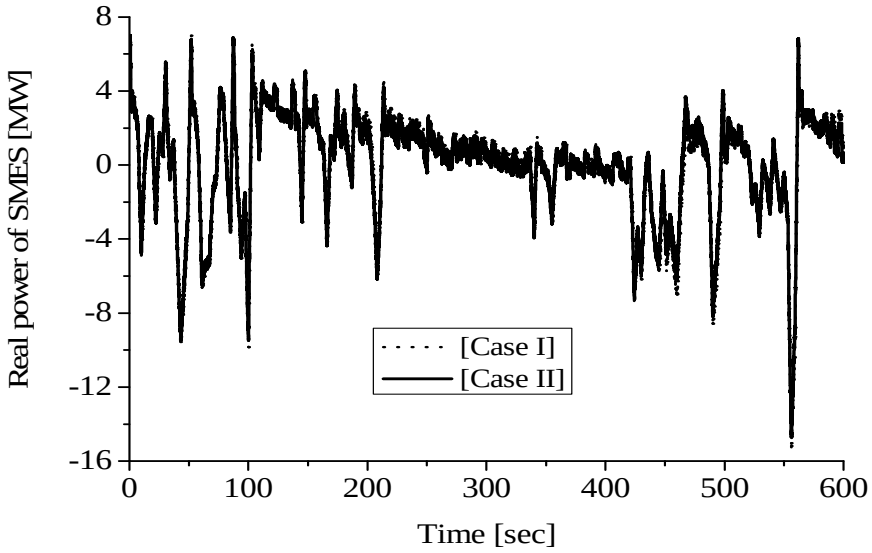

Fig. 23. Responses of SMES real power

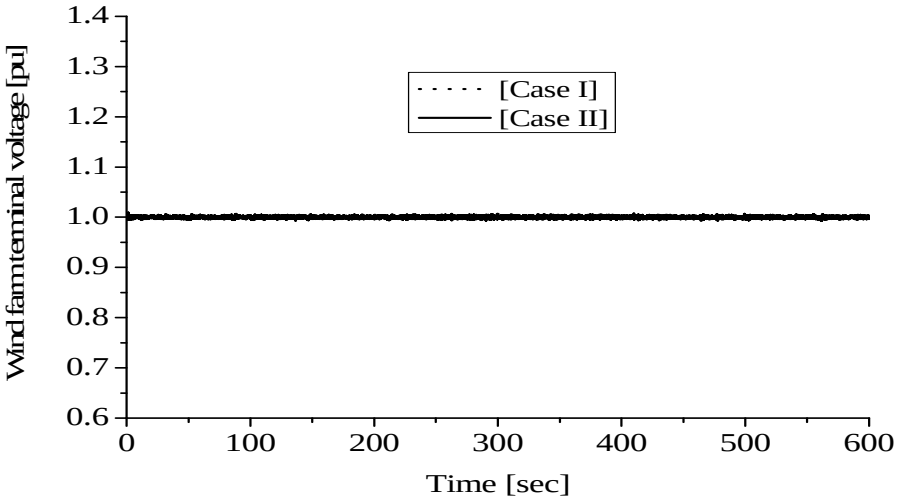

Fig. 24. Responses of WF terminal voltage with STATCOM/SMES

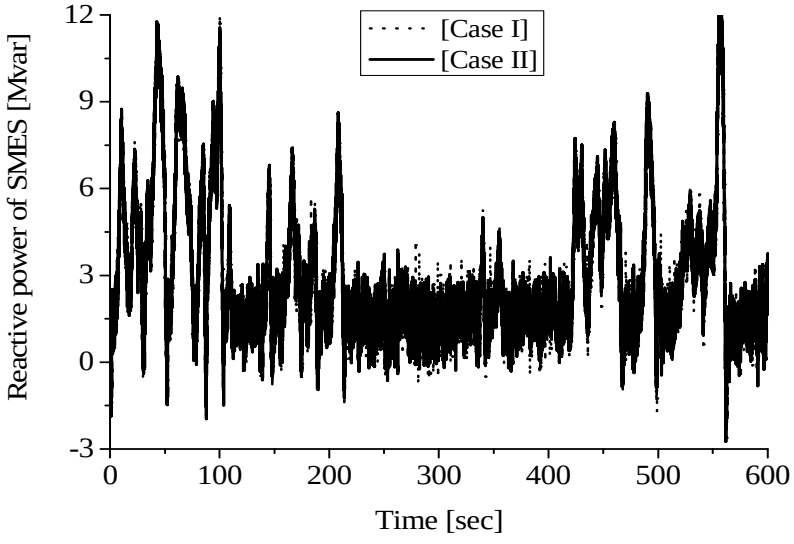

Fig. 25. Responses of SMES reactive power

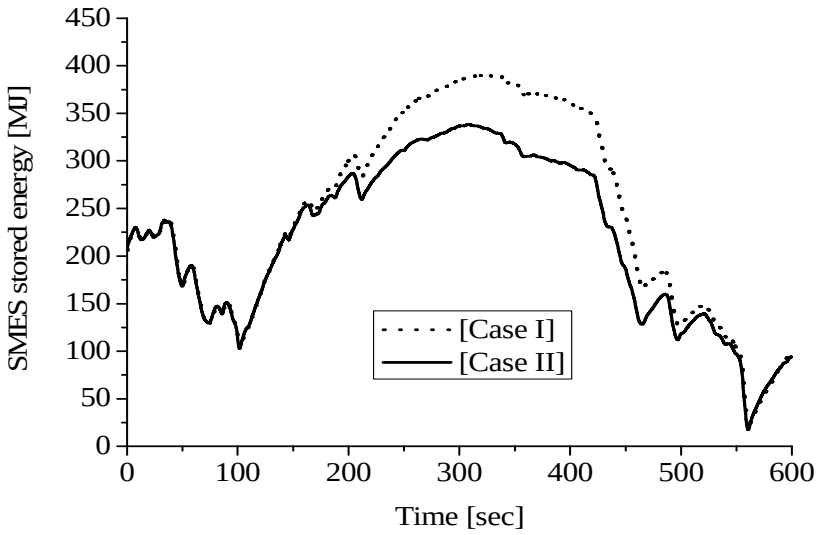

Fig. 26. Responses of SMES stored energy

Fig. 25 and Fig. 26 show the responses of SMES reactive power and SMES stored energy respectively. It is also clear from Fig. 25 and Fig. 26 that more reactive power compensation and larger SMES energy storage capacity are needed in case I than Case II.

7. Conclusions

In this study, the control scheme of STATCOM/SMES topology for wind power application is presented. Two wind speed patterns are used to simulate the results. As wind is fluctuating in nature, the output power and terminal voltage of wind generator also fluctuate randomly. The effectiveness of the proposed STATCOM/SMES topology on smoothing the wind farm output power and terminal voltage is investigated, in which both SMA and EMA are used to generate output power reference. It is seen that the proposed control system can smooth the wind farm output power as well as maintain constant voltage magnitude at wind farm terminal in both cases with the two power references used. But comparatively larger SMES real power and reactive power compensation and also more energy storage capacity are needed in the case with SMA used. These comparisons are visualizing more when wide variations of wind speed pattern are used. Finally, it can be concluded that the proposed STATCOM/SMES topology is more effective to minimize the output power fluctuations of wind farm and decrease the terminal voltage deviations.

References:

[1] S. Morozumi, Present state future on electric power storage "Distributed electricity-generation of output fluctuation control by energy storage system", Electric Review, pp.44-48, 2006.12.

[2] L. Zhang, C. Shen, M. L. Crow, L. Dong, S. Pekarek, and S. Atcitty, "Performance Indices for the Dynamic Performance of FACTS and FACTS with Energy Storage," *Electric Power Component and System*, Vol.33, No.3, pp.299-314, March 2005.

[3] S.M. Muyeen, S. Shishido, M.H. Ali, R. Takahashi, T. Murata, and J.Tamura, "Application of Energy Capacitor System (ECS) to Wind Power Generation", *Wind Energy*, Vol. 11, No. 4, pp. 335-350, DOI: 10.1002/we.265, July/August 2008.

[4] R. S. Bhatia, S. P. Jain, D. K. Jain, and B. Singh, "Battery Energy Storage System for Power Conditioning of Renewable Energy Sources," International Conference on Power Electronics and Drive Systems (*IEEE PEDS 2005)*, Conference CDROM, pp. 501-506, Malaysia, 2005.

[5] T. Nitta, "Present state and future on electric power storage. Could superconducting magnetic energy storage system (SMES) be realized?", IEEJ journal, Vol.123, No.5, pp.278-279, 2003

[6] F. Irie, "The state of the art of superconducting magnetic energy storage system (SMES)", IEEJ, Vol.116-B, No.9, pp.1029-1032, 1996

[7] N. Hirano, S. Nagaya, Present state future on electric storage "Development trend of Superconducting Magnetic Energy Storage", Electric Review, pp.26-31, 2006.12.

[8] H. J. Boenig and J. F. Hauer, "Commissioning Tests of the Bonneville Power Administration 30 MJ Superconducting Magnetic Energy Storage Unit," *IEEE Transaction on Power Apparatus and Systems*, Vol. PAS-104, No. 2, pp. 302-309, February 1985.

[9] M.R.I. Sheikh, S.M. Muyeen, Rion Takahashi, Toshiaki Murata and Junji Tamura, "Minimization of Fluctuations of Output Power and Terminal Voltage of Wind Generator by Using STATCOM/SMES", *2009 IEEE Bucharest PowerTech Conference*, June 28th - July 2nd., Bucharest, Romania.

[10] M. H. Ali, T. Murata, and J. Tamura, "A Fuzzy Logic-Controlled SMES for Damping Shaft Torsional Oscillations of Synchronous Generator ", IEEJ Trans, Vol.1 No.1 Page.116-120, 2006.05.
[11] IEEE Task Force on Benchmark Models for Digital Simulation of FACTS and Custom–Power Controllers, T&D Committee, "Detailed Modeling of Superconducting Magnetic Energy Storage (SMES) System", *IEEE Trans. Power Delivery*, Vol. 21, No. 2, pp. 699-710, April 2006.
[12] M.R.I. Sheikh, S.M. Muyeen, Rion Takahashi, Toshiaki Murata and Junji Tamura "Transient Stability Enhancement of Wind Generator Using Superconducting Magnetic Energy Storage Unit", *International Conference of Electrical Machine (ICEM, 08)*, Conference CD (Paper ID-1027), 06-09 September, 2008, Portugal.
[13] S.M. Muyeen, Mohd. Hasan Ali, Rion Takahashi, Toshiaki Murata, and Junji Tamura, "Transient Stability Enhancement of Wind Generator by a New Logical Pitch Controller*",* *IEEJ Transaction on PE*, Vol.126, No.8, 2007, pp. 742-751.
[14] C.L. Souza, L.M. Neto, G.C. Guimaraes, and A.J. Moraes, "Power System Transient Stability Analysis Including Synchronous and Induction Generator", *IEEE Porto Power Tech. Proceddings*, Vol.2, p.6(2001).
[15] S.M. Muyeen, T. Murata, and J.Tamura, "Stability Augmentation of Grid Connected Wind Farm", *Springer Verlag-London*, October, 2008.
[16] S.Heier: Grid Integration of Wind Energy Conversion System, *John Wiley & Sons Ltd*., Chicester, UK(1998)
[17] O. Wasynczuk, D. T. Man, J. P. Sullivan, "Dynamic behavior of a class of wind turbine generator during random wind fluctuations," IEEE Trans. on Power Apparatus and Systems, Vol. PAS-100, No.6, pp.2873-2845, 1981.
[18] D. Driankov, H. Hellendoorn, and M. Reinfrank: An Introduction to Fuzzy Control, Springer-Verlag (1993).
[19] PSCAD/EMTDC Manual, *Manitoba HVDC Research Center* (1994).

M.R.I. Sheikh was born in Sirajgonj, Bangladesh on October 31, 1967. He received his B.Sc. Engineering and M.Sc. Engineering Degrees from Rajshahi University of Engineering & Technology (RUET), Bangladesh, in 1992 and 2003 respectively, all in Electrical and Electronic Engineering. He carryout his Ph.D degree from Kitami Institute of Technology, Hokkaido, Kitami, Japan in 2010 in the field of Renewable Wind Energy. He published more than seventy papers including Transactions, Journal and International Conferences. He was the Editor of the book Energy Storage. He also published two book chapters. He is recently working to publish a book based on his research in Wind Energy. He is currently Professor and working as the Head of Electrical and Electronic Engineering Department, RUET. His research interests are, Power system stability enhancement including wind generator by using SMES, FACTs devices and Load Frequency Control of multi-area power system. Mr. Sheikh is the member of the IEB and the BCS of Bangladesh.

Junji Tamura received his B. Sc. Eng. Degree from Muroran Institute of Technology, Japan, in 1979 and M.Sc. Eng. and Dr. Eng. degrees from Hokkaido University, Japan, in 1981 and 1984 respectively, all in electrical engineering. In 1984, he became a lecturer and in 1986, an associate professor at the Kitami Institute of Technology, Japan. Currently he is a professor at the Kitami Institute of Technology. Dr. Tamura is a member of IEE of Japan and a senior Member of the IEEE Power Engineering Society.